ACS APPLIED MATERIALS & INTERFACES

Research Article

www.acsami.org

Core–Shell–Corona-Structured Polyelectrolyte Brushes-Grafting Magnetic Nanoparticles for Water Harvesting

Guoqiang Liu,[†,‡] Meirong Cai,[†] Xiaolong Wang,*[,†] Feng Zhou,*[,†] and Weimin Liu[†]

[†]State Key Laboratory of Solid Lubrication, Lanzhou Institute of Chemical Physics, Chinese Academy of Sciences, Lanzhou 730000, China

[‡]University of Chinese Academy of Sciences, Beijing 100039, China

Supporting Information

ABSTRACT: A novel superhydrophilic material, charged polymer brushes-grafted magnetic core–shell–corona composite nanoparticles (Fe_3O_4@SiO_2@PSPMA), was developed to harvest water through the hydration effect. Because of both the strong hydration capability and the good swelling performance, the negatively charged polymer brushes, PSPMA brushes, endow the composite nanoparticles with superhydrophilicity and a good water-absorbing performance like a sponge, while the magnetic Fe_3O_4 cores allow easy separation of Fe_3O_4@SiO_2@PSPMA nanoparticles with absorbed water from oil/water mixture under an external magnetic field. The functional particles have the capability of harvesting water droplets whether floating on an oil surface or in the oil. This water-absorbing material uses selective wettability to harvest water and achieve oil–water separation and may be useful in finding novel approaches for recycling water from sewage and removing water in the petroleum industry.

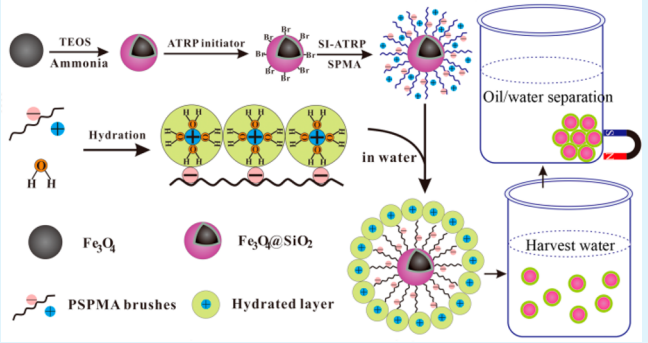

KEYWORDS: *charged polymer brushes, Fe_3O_4@SiO_2@PSPMA, magnetic nanoparticles, hydration effect, water harvesting, oil–water separation*

1. INTRODUCTION

With increasing environmental pollution and water shortage, novel strategies to harvest and separate water from oil–water mixture are highly desired. Since water harvesting and oil/water separation is an interfacial problem, it is an effective and a simple strategy to design novel materials with special wettability.[1−3] For oil/water separation, "oil-absorbing" types of materials with both superhydrophobic and superoleophilic properties have been widely used to filtrate or absorb oils from water effectively.[4−6] However, oil-absorbing materials are easily fouled by oils, and oils adhered are difficult to remove, leading to the marked decrease of separation efficiency as well as the secondary pollution.[7] In practical applications, it may be an alternative strategy to design "water-absorbing" materials for harvesting water and achieving oil/water separation. In comparison with traditional oil-absorbing materials, this novel water-absorbing material has completely opposite wettability and thus overcomes the easy-fouling limitation.[8−10] Currently, oil–water separation methods mostly focus on the design of hierarchical structure.[11−13] Herein, we develop a new method to achieve oil–water separation, which depends on the hydration effect induced by a large electric dipole. When the composite nanoparticles were exposed to the water droplets in an oil–water mixture, they swelled strongly and absorbed the water droplets like a sponge.

Water molecules can form hydration layers surrounding charges in aqueous media, which is attributed to the large electric dipole by virtue of the residual charges on the H and O atoms.[14,15] Such a hydration layer greatly lowers the self-energy of the entrapped charge, that is, it can be very difficult to permanently remove a water molecule from the hydration layer surrounding a charge.[16,17] In this case, water molecules were still firmly absorbed around a charge in spite of vigorous shock during the practical oil–water separation process. Magnetic polymeric nanoparticles, a promising advanced composite material, have attracted tremendous attention owing to their unique magnetic responsiveness and their potential applications in various fields, such as bioseparation,[18−21] magnetically targeted drug delivery,[22,23] and magnetic resonance imaging.[24−26] In particular, designing functional magnetic polymeric nanoparticles with special wettability is of great concern in the field of oil/water separation.[27] Therefore, charged polymer brushes-grafted magnetic nanoparticles were prepared herein to combine the advantages of charged polymer brushes on the hydration effect and magnetic nanoparticles on facile separation and large surface area, making our present core–shell–corona nanoparticles promising oil–water separation materials.[28−30] As

Received: April 21, 2014
Accepted: June 23, 2014
Published: June 23, 2014

Scheme 1. Illustration of the Synthetic Procedure for the Charged Polymer Brushes-Grafted Magnetic Core−Shell−Corona Composite Nanoparticles (Fe_3O_4@SiO_2@PSPMA), Hydration Mechanism of PSPMA Brushes, and Procedure for Water Harvesting and Oil/Water Separation

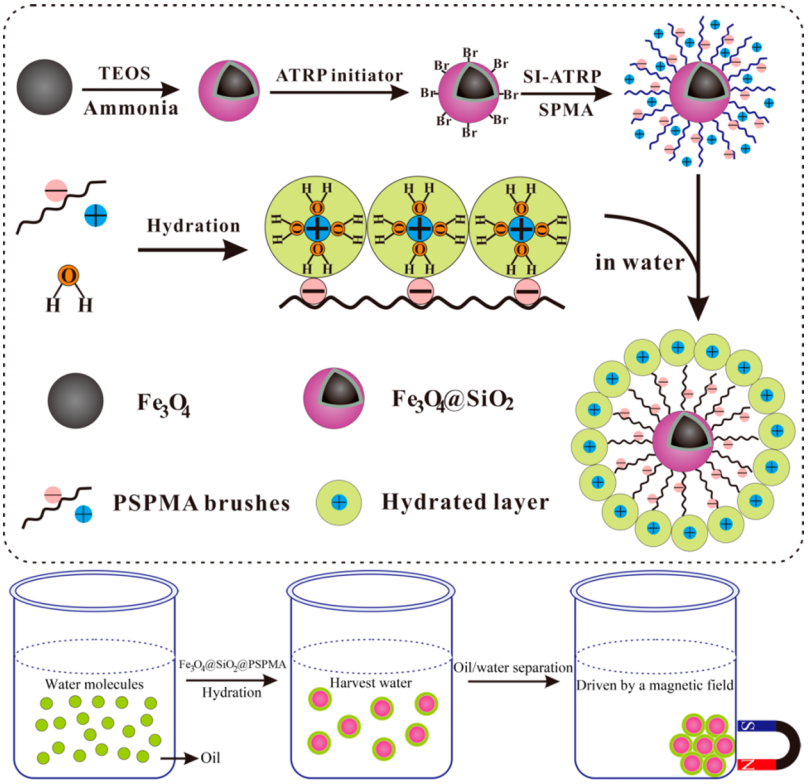

proof-of-concept, negatively charged poly(3-sulfopropyl methacrylate potassium salt) (PSPMA) brushes-grafted Fe_3O_4@SiO_2 composite nanoparticles were prepared. PSPMA brushes possess strong hydration capability in aqueous media[31,32] that can harvest water droplets in an oil−water mixture. Use of a silica coating is to protect Fe_3O_4 cores from damage and aggregation and supplies a suitable supporting matrix to immobilize functional groups owing to numerous surface Si−OH groups.[33−36] When the composite magnetic nanoparticles were put into an oil−water mixture, the dispersed water was gathered together to form hydrated liquid marbles, and then the marbles could freely move using an external magnetic field to realize separation.

2. EXPERIMENTAL SECTION

2.1. Materials. Ferric chloride hexahydrate ($FeCl_3·6H_2O$), ethylene glycol (EG), anhydrous sodium acetate, and ammonium hydroxide (25−28%) and methyl blue were purchased from Sinopharm Chemical Reagent Co., Ltd. (China). Tetraethyl orthosilicate (TEOS, 98%) was purchased from Sigma-Aldrich. 3-(Trichlorosilyl)propyl-2-bromo-2-methylpropanoate (initiator ATRP-Br) was synthesized in our lab.[37−39] 3-Sulfopropyl methacrylate potassium salt (98%, SPMA), 2,2′-bipyridine (Bpy, 99%), and copper(I) bromide (CuBr) were purchased from TCI Co., Ltd. CuBr was refluxed with acetic acid prior to use. Toluene was purified by distillation over CaH_2. Other chemicals were used as received. Deionized water was used for all polymerization and treatment processes.

2.2. Synthesis of Fe_3O_4 Magnetic Nanoparticles. Fe_3O_4 magnetic nanoparticles were prepared through a modified solvothermal reaction.[40] Briefly, 1.35 g of $FeCl_3·6H_2O$, 3.6 g of sodium acetate, and 0.4 g of sodium citrate were dissolved in 50 mL of ethylene glycol via stirring. The obtained homogeneous yellow solution was then sealed in a Teflon-lined stainless-steel autoclave (100 mL) and heated at 200 °C for 12 h. After being cooled to room temperature, the obtained black magnetite particles were collected, washed with ethanol several times, and finally dried in vacuum at 40 °C for 24 h.

2.3. Synthesis of Fe_3O_4@SiO_2 Core−Shell Nanoparticles. Fe_3O_4@SiO_2 core−shell nanoparticles were prepared according to the method previously reported with slight modification.[41] Typically, 50 mg of Fe_3O_4 nanoparticles was dispersed in a mixture of 40 mL of ethanol and 10 mL of water by ultrasonication for 20 min. Then under continuous mechanical stirring, 1.5 mL of ammonia solution (25−28 wt %) was added to the mixture, followed by 0.3 mL of TEOS being added dropwise. After being kept at room temperature for 6 h, the solid products were collected using an external magnet, rinsed with water and ethanol, and dried in a vacuum oven at 40 °C for 12 h.

2.4. Immobilization of ATRP Initiator. Fe_3O_4@SiO_2 nanoparticles (25 mg) were stirred at room temperature for 24 h in the anhydrous toluene solution (25 mL) containing 10 μL of 3-(trichlorosilyl)propyl 2-bromo-2-methylpropanoate. The hydrolysis/condensation process between the ATRP initiator and silica resulted in the immobilization of initiator. Then the initiator-immobilized Fe_3O_4@SiO_2 nanoparticles were collected by a magnet, washed several times with fresh anhydrous toluene and ethanol, and dried in vacuum at room temperature for 24 h.

2.5. Synthesis of PSPMA Brushes-Grafted Fe_3O_4@SiO_2 Composite Nanoparticles by Surface-Initiated ATRP. Typically, the initiator-immobilized Fe_3O_4@SiO_2 nanoparticles (10 mg) and SPMA (1.5 g) were dispersed in 1:4 (v:v) MeOH/H_2O (10 mL) via 10 min of ultrasonication. After being deoxygenated for 30 min at room temperature using nitrogen flow, 2,2′-bipyridyl (0.0625 g, 0.4 mmol) and CuBr (0.0287 g, 0.2 mmol) were added into the dispersion quickly to trigger polymerization. Polymerization was conducted at room temperature under N_2 protection for 2 h. Finally, PSPMA brushes-grafted Fe_3O_4@SiO_2 composite nanoparticles were collected by a magnet, washed several times with deionized water and ethanol, and dried in a vacuum oven at room temperature for 24 h.

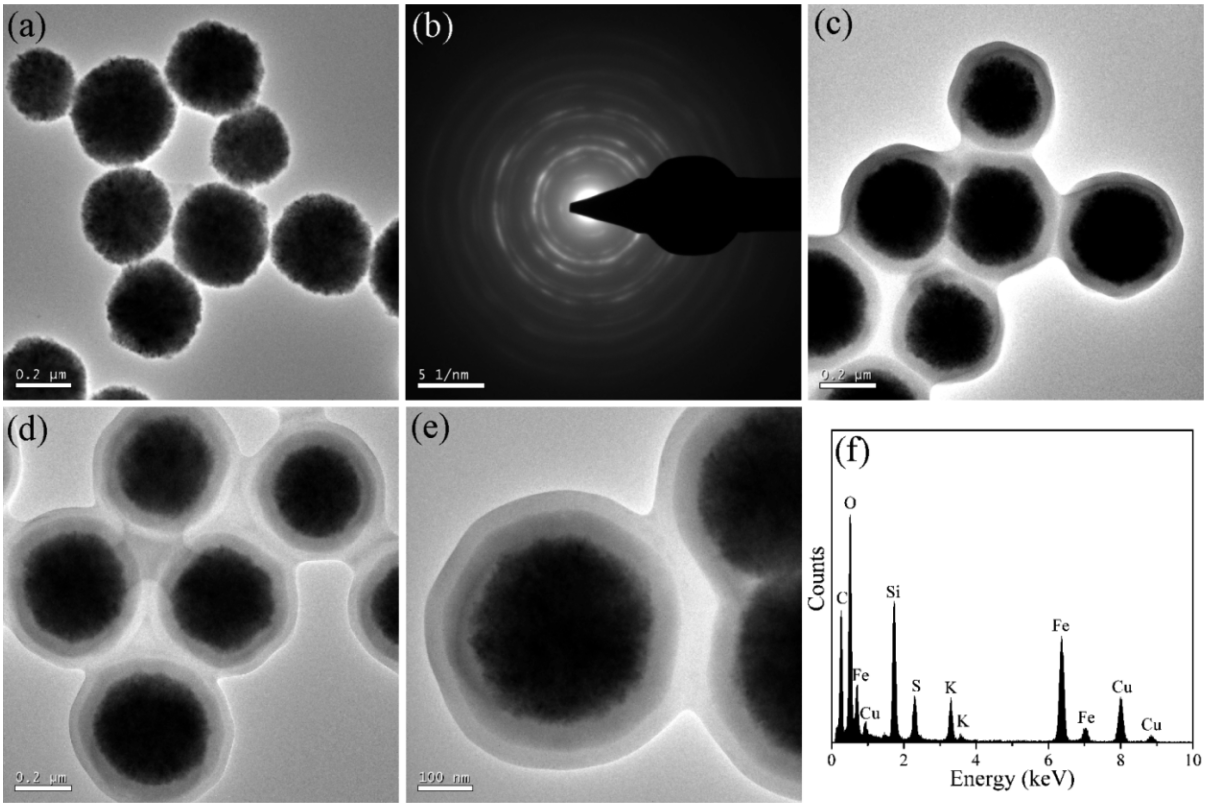

Figure 1. TEM image (a) and SAED pattern (b) of Fe_3O_4 nanoparticles; TEM images of Fe_3O_4@SiO_2 core−shell particles (c) and Fe_3O_4@SiO_2@PSPMA composites (d, e); EDXS spectra of Fe_3O_4@SiO_2@PSPMA composites (f).

2.6. Water Harvesting and Oil/Water Separation. Scheme 1 illustrates the procedure for water harvesting and oil/water separation. Water droplets were dyed blue by methyl blue. For the water droplet floating on the oil surface, the composite particles were placed on the water droplet. After a water-absorbing process (about 30 s), the particles/water marble formed and was driven by a regular magnet. For the water droplets under oil, the magnetic particles were added into the oil/water mixture and shaken vigorously. After formation of particles/water marble, the marble was moved to the magnet responsively.

2.7. Characterization. Transmission electron microscopy (TEM) images were obtained from a FEI Tecnai G2 TF20 transmission electron microscope with a field emission gun operating at 200 kV. The elemental composition was evaluated using energy-dispersive X-ray spectroscopy (EDXS). Fourier transform infrared (FT-IR) spectra were determined on a Nicolet iS10 (Thermo Scientific, USA) FT-IR spectrometer. Thermogravimetric analysis (TGA) was performed on a STA 449C TG-DSC instrument. X-ray diffraction (XRD) measurements were carried out on a PANalytical X'Pert PRO X-ray diffractometer with Cu Kα (λ = 0.15418 nm) incident radiation. Magnetic properties were studied on a vibrating sample magnetometer (VSM) on a model 6000 physical property measurement system (Quantum, USA) at 300 K. Hydrodynamic diameters (D_h) and zeta potential were measured on a particle size analyzer (Zetasizer Nano ZS, Malvern Instruments, UK) equipped with a 632.8 nm He−Ne laser by dynamic light scattering (DLS) technique. The swelling ratio (SR) was deremined by the following equation: SR = $V_{aqueous}/V_{dry}$ = (D_h/D_{dry}),[3] where $V_{aqueous}$ and V_{dry} were the volumes in aqueous media and in the dry state, respectively, and $D_{aqueous}$ and D_{dry} were the mean diameters from DLS and TEM, respectively. The resulting composite particles were deposited on a microfiltration membrane (pore size 220 nm) by filtration and dried and form a dense and thick film. The water contact angle on the deposited film was measured with a 5 μL droplet of distilled water at ambient temperature with a DSA100 contact angle (CA) meter (Kruss Co., Germany). The oil contact angle on the deposited film was tested using a 5 μL droplet of dichloromethane dyed by oil red in water. In the reusability test, 10 mg of the nanocomposites and 30 mg of water were adopted. The used nanocomposites were centrifuged and dried before the next cycle. KCl solutions with different concentrations were employed to investigate the effect of ionic strength on the nanocomposites. PBS buffer solutions with a pH value from 2 to 14 were prepared to investigate the effect of pH on the nanocomposites.

3. RESULTS AND DISCUSSION

3.1. Synthesis and Characterization of Fe_3O_4@SiO_2@PSPMA Nanoparticles. The procedure for preparation of PSPMA brushes-grafted Fe_3O_4@SiO_2 core−shell−corona composite nanoparticles (Fe_3O_4@SiO_2@PSPMA) is illustrated in Scheme 1. Briefly, magnetic Fe_3O_4 NPs were first prepared via a solvothermal reaction. Then, the Fe_3O_4 NPs were encapsulated by a SiO_2 shell through a sol−gel process. Finally, core−shell−corona structured nanoparticles, PSPMA brushes-grafted Fe_3O_4@SiO_2, were obtained via immobilizing Br-containing initiator, followed by surface-initiated ATRP of SPMA.

Representative morphology of the as-prepared particles (Fe_3O_4, Fe_3O_4@SiO_2, and Fe_3O_4@SiO_2@PSPMA) was observed by TEM, which verifies the synthetic procedure illustrated in Scheme 1, as shown in Figure 1. It showed that the Fe_3O_4 particles prepared via solvothermal reaction were nearly spherical in shape with mean diameter of ca. 356 nm (Figure 1a). The magnetite exhibits polycrystalline features that were confirmed by spotty diffraction rings of selected area electron diffraction pattern (Figure 1b). Then, as observed by the TEM image in Figure 1c, a layer of dense amorphous silica with a thickness of ca. 55 nm was successfully coated on the

Fe_3O_4 particles via the sol−gel process, resulting in the magnetic core−shell Fe_3O_4@SiO_2 microspheres. Afterward, the surface-initiated ATRP resulted in a core−shell−corona structure of Fe_3O_4@SiO_2@PSPMA (Figure 1d). The magnified image shown in Figure 1e evidently reveals a dark Fe_3O_4 core, a gray SiO_2 middle shell, and a light-gray PSPMA corona about 42 nm in thickness. Successful grafting of PSPMA brushes on the surface of Fe_3O_4@SiO_2 was also confirmed by the EDXS measurement (Figure 1f), which shows the appearance of S and K signals attributed to the PSPMA.

Successful preparation of Fe_3O_4@SiO_2@PSPMA was also confirmed by FTIR spectroscopy (Figure 2). For Fe_3O_4 NPs

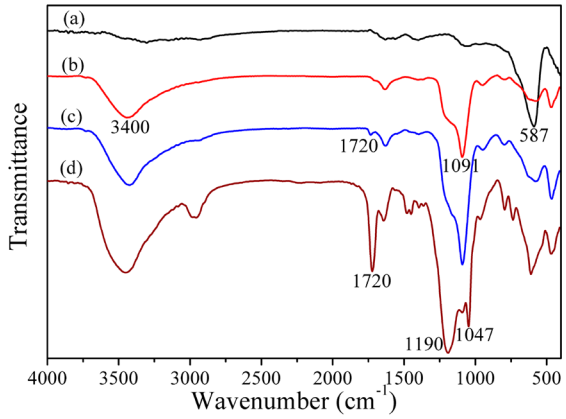

Figure 2. FTIR spectra of (a) Fe_3O_4, (b) Fe_3O_4@SiO_2, (c) Fe_3O_4@SiO_2−Br, and (d) Fe_3O_4@SiO_2@PSPMA.

(Figure 2a), the absorption peak at 587 cm^{-1} was assigned to Fe−O absorption. For Fe_3O_4@SiO_2 (Figure 2b), the absorption peak of Si−O−Si appeared at 1091 cm^{-1} whereas the wide peak at 3400 cm^{-1} was assigned to the stretching absorption vibration of Si−OH. After modification with ATRP initiator, some new peaks were observed from Fe_3O_4@SiO_2−Br (Figure 2c). The peaks at 1720 and 2940 cm^{-1} can be assigned to the ester C═O and C−H bonds from the silane initiator. After the PSPMA brushes were grafted from the surface of Fe_3O_4@SiO_2−Br via SI-ATRP, the characteristic absorption peaks of S═O in SO_3^- groups appeared at 1190 and 1047 cm^{-1}, whereas the strong absorption peak at 1720 cm^{-1} appeared from C═O in ester groups (Figure 2d). The appearance of these absorption peaks confirmed that polymer brushes have been grafted onto Fe_3O_4@SiO_2−Br.

To quantitatively determine the composite of the obtained Fe_3O_4@SiO_2@PSPMA, thermogravimetric analysis was conducted. Figure 3 showed the TGA curves of the obtained Fe_3O_4, Fe_3O_4@SiO_2, Fe_3O_4@SiO_2−Br, and Fe_3O_4@SiO_2@PSPMA, and the weight loss was evaluated from 50 to 800 °C. The weight loss of Fe_3O_4 was 3.8 wt %, which was attributed to degradation of the stabilizer sodium citrate (Figure 3a). A weight loss of 6.9 wt % was observed from the curve of Fe_3O_4@SiO_2 (Figure 3b), which was related to water molecules bonded to SiO_2. After immobilization of ATRP initiator, the weight loss of Fe_3O_4@SiO_2−Br was 9.7 wt % (Figure 3c) and the content of the initiator was calculated to be 2.8 wt %. Moreover, after being grafted with PSPMA brushes by ST-ATRP, the weight loss of composite particles was increased to 33.8 wt %, indicating the content of PSPMA brushes was 24.1 wt % (Figure 3d). Notably, from the TGA curve of Fe_3O_4@SiO_2@PSPMA there were two obvious decomposition steps. The first

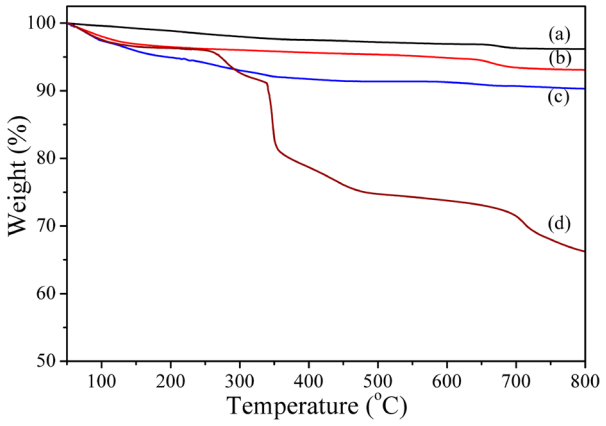

Figure 3. TGA curves (a) of Fe_3O_4, (b) Fe_3O_4@SiO_2, (c) Fe_3O_4@SiO_2−Br, and (d) Fe_3O_4@SiO_2@PSPMA.

step at around 300 °C was derived from conventional thermal decomposition of a majority of PSPMA brushes. The second step at around 680 °C was attributed to the weight loss of partial PSPMA brushes that were directly attached to the surface of Fe_3O_4@SiO_2 nanoparticles. The second decomposition step reflects the strong attachment between Fe_3O_4@SiO_2 and PSPMA brushes, which is similar to previous reports.[19,42,43]

Crystal structures of the as-prepared Fe_3O_4, Fe_3O_4@SiO_2, and Fe_3O_4@SiO_2@PSPMA were also investigated by X-ray diffraction (XRD) and are shown in Figure 4.The diffraction

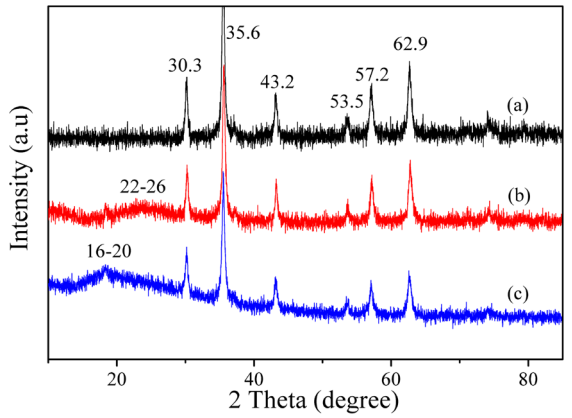

Figure 4. XRD patterns for (a) Fe_3O_4, (b) Fe_3O_4@SiO_2, and (c) Fe_3O_4@SiO_2@PSPMA.

peaks can be indexed to the face-centered cubic structure of magnetite according to JCPDS.[44] Six characteristic peaks (2θ = 30.3°, 35.6°, 43.2°, 53.5°, 57.2°, and 62.9°) related to their corresponding indices ((220), (311), (400), (422), (511), and (440)) were observed in the case of the Fe_3O_4 magnetic particles (Figure 4a). Then, for an XRD pattern of the Fe_3O_4@SiO_2 (Figure 4b), a broad peak at 2θ of 22−26° corresponded to the amorphous peak of SiO_2. Furthermore, after the coverage of PSPMA brushes, another broad diffusion pattern of amorphous polymer layer appeared at 2θ of 16−20° in the XRD pattern of Fe_3O_4@SiO_2@PSPMA (Figure 4c).

3.2. Magnetic Property of the As-Prepared Nanoparticles. The magnetic property of the as-prepared nanoparticles was investigated by a vibrating sample magnetometer at room temperature. Figure 5 showed the magnetic hysteresis

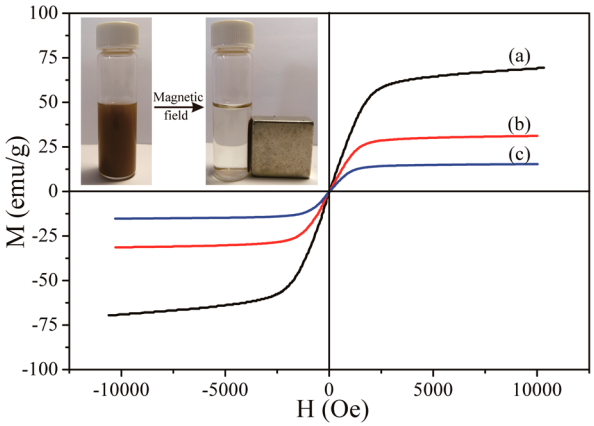

Figure 5. Magnetic hysteresis loops of (a) Fe_3O_4, (b) Fe_3O_4@SiO_2, and (c) Fe_3O_4@SiO_2@PSPMA. (Inset) Picture of Fe_3O_4@SiO_2@PSPMA gathered and driven by a regular magnet in water.

loops of Fe_3O_4, Fe_3O_4@SiO_2, and Fe_3O_4@SiO_2@PSPMA, which exhibited superparamagnetic behavior and no obvious remanence and coercivity.[45] The magnetic saturation (M_s) values were 69.5, 31.3, and 15.2 emu/g, respectively. The M_s values of Fe_3O_4@SiO_2 and Fe_3O_4@SiO_2@PSPMA are both lower than that of Fe_3O_4, which is due to the decrease in the density of Fe_3O_4 in the obtained nanocomposites after coverage of nonmagnetic SiO_2 and grafting of nonmagnetic PSPMA brushes. It should be noted that the resulting composite nanoparticles still showed strong magnetization, which suggested their suitability for magnetic separation and targeting using a regular magnetic plate (Figure 5, inset).

3.3. Hydration Capability of Fe_3O_4@SiO_2@PSPMA Nanocomposites. To investigate the hydration capability of PSPMA brushes, the hydrodynamic diameter and zeta potential of Fe_3O_4@SiO_2@PSPMA particles was measured using DLS in aqueous media. As shown in Figure 6a, the intensity-average hydrodynamic diameter of Fe_3O_4@SiO_2@PSPMA (ca. 864 nm) was much larger than the size obtained in the TEM images (ca. 550 nm). Correspondingly, the swelling ratio ($V_{aqueous}/V_{dry}$) was calculated to be 3.88. Because the ionic PSPMA polymer chains could be fully extended in aqueous media, Fe_3O_4@SiO_2@PSPMA composites possessed a good swelling capability like a sponge. On the basis of the hydration mechanism illustrated in Scheme 1, water molecules could form hydrated layer surrounding a charge. To lower the born energy of the encapsulated polar groups, the hydrated layer was robust and difficult to be removed. As shown in Figure 6b, the zeta potential of Fe_3O_4@SiO_2@PSPMA particles is −53.2 mV, suggesting a strong hydration capability of negatively charged PSPMA brushes. Additionally, because of electrical interaction, the hydrodynamic size and zeta potential distribution both exhibited a single peak, indicating a good dispersibility of the resultant composites in aqueous media.

Due to the strong hydration capacity and good swelling performance of PSPMA brushes, the Fe_3O_4@SiO_2@PSPMA composites exhibited special wettability. As shown in Figure 6c and Video S1 (Supporting Information), the contact angle (CA) of the water dropped on the Fe_3O_4@SiO_2@PSPMA film was reduced to 0° within ca. 25 s, suggesting a superhydrophilic performance of Fe_3O_4@SiO_2@PSPMA nanoparticles. Interestingly, the water droplet permeated into the interior of the film quickly rather than spreading on the film, which demonstrates that the as-prepared composite nanoparticles possess strong water-absorbing capability. This phenomenon was attributed to the strong hydration effect and good swelling performance of the outermost PSPMA brushes. In addition to the strong water-absorbing capability, the wettability of the Fe_3O_4@SiO_2@PSPMA film for oil under water was also investigated. As shown in Figure S1 (Supporting Information), the contact angle of dichloromethane on the film underwater was 165 ± 3°, indicating a superoleophobic property. Thus, in oil/water mixture, the nanocomposites can be fast wetted by water instead of oil. Moreover, since the PSPMA brushes-grafted Fe_3O_4@SiO_2 nanoparticles possess a strong magnetic core and a superhydrophilic PSPMA exterior, they hold great promise for rapid magnetic separation of water in oil/water systems.

3.4. Water Harvesting and Oil−Water Separation. On the basis of its selective wettability, the obtained PSPMA brushes-grafted magnetic particles were used to absorb water from oil−water mixture, and the schematic diagram is illustrated in Scheme 1. In general, the distribution of water droplets in the oil has two modes: one is the water droplets floating on the oil surface; the other is the water droplets under

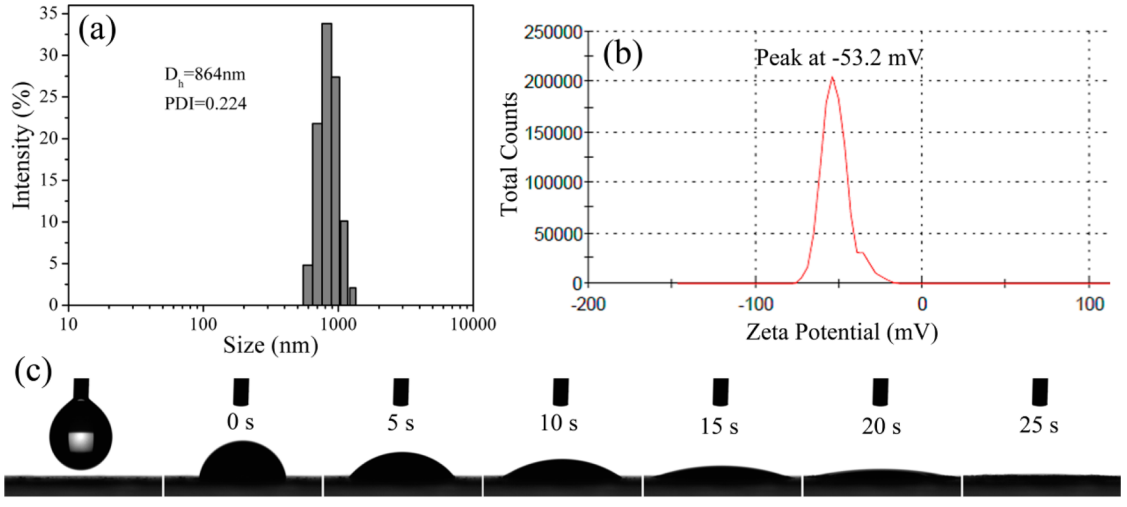

Figure 6. (a) Hydrodynamic diameter distribution of Fe_3O_4@SiO_2@PSPMA particles. (b) Zeta-potential distribution of Fe_3O_4@SiO_2@PSPMA particles. (c) Changing contact angel of water on the deposited film of Fe_3O_4@SiO_2@PSPMA particles with time.

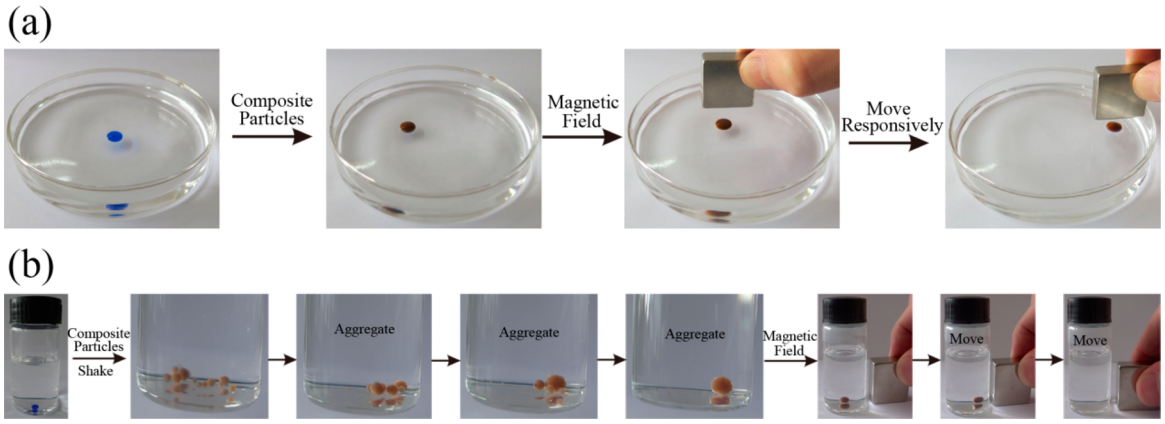

Figure 7. Water harvesting and oil/water separation procedures for the water droplets floating on dichloromethane surface (a) and the water droplets under hexane (b).

oil. Hopefully, the two types of water droplets are both harvested by the as-prepared composite magnetic particles.

Dichloromethane/H_2O mixture was chosen to investigate the ability of the as-prepared composite nanoparticle to harvest the water droplets floating on the oil surface. As shown in Figure 7a, a drop of water, which has been dyed blue, was dropped on the oil surface, and then the superhydrophilic magnetic particles were added and spread in the water. Due to the high hydration capability of PSPMA brushes, the water was absorbed and surrounding the PSPMA brushes-grafted magnetic particles. Subsequently, the particle/water marble was formed. When putting a magnet close by, the water-holding magnetic particles moved along with the magnet responsively. Fortunately, these particles can be recycled by centrifugation. Additionally, the isolated water-holding magnetic nanoparticles could be gathered together and removed through the magnet (Video S2, Supporting Information), which broadened the range of water collection. Using a certain amount of nanocomposites (10 mg), up to 50 mg of water can be absorbed and removed by a magnet. Besides, the reusability of the nanocomposites was studied by a cycle test. The used nanocomposites was first centrifuged and dried. As shown in Table S1 (Supporting Information), in spite of a small loss, the water harvesting process of the dried nanocomposites can be successfully cycled.

Furthermore, hexane/water mixture was chosen to test the absorption capability of the as-prepared composite nanoparticles to harvest the water droplets under oil. As shown in Figure 7b, a drop of water, which has been dyed by methyl blue, was dropped into the hexane. Then the magnetic particles were added into the oil/water mixture and shaken vigorously. Afterward, the small dispersed water droplets were absorbed around the PSPMA brushes-grafted magnetic particles. Interestingly, the small dispersed PSPMA brushes-grafted magnetic particles with absorbed water can gather together and form a big magnetic bead through a slight shaking, which may be attributed to the high surface energy of Fe_3O_4@SiO_2@PSPMA nanoparticles, easily triggering aggregation of the nanoparticles. Due to its magnetic property, the PSPMA brushes-grafted magnetic particles with absorbed water could also be facilely moved under external magnetic control. When putting a magnet close by, the magnetic bead moved toward the magnet responsively. In addition, the isolated water-holding magnetic beads, which were formed by vigorous shaking, could gather together fast through liquid–liquid separation (Video S3, Supporting Information). Notably, the "water marble" was spherical and could roll freely under the consideration of minimizing the surface free energy (Video S4, Supporting Information). These results demonstrated that the water droplets could be easily harvested by Fe_3O_4@SiO_2@PSPMA and separated using a regular magnet.

To investigate the effect of ionic strength and pH on the water-absorbing materials for harvesting water, the hydrodynamic size of Fe_3O_4@SiO_2@PSPMA nanocomposites under various ionic strength and pH was first measured by DLS. As shown in Figure S2 (Supporting Information), the hydrodynamic diameter decreased gradually with increasing concentration of KCl solution, whereas the hydrodynamic diameter had no obvious change with pH value. The conformation transition of polyelectrolyte brushes can be adjusted by different pH and ion strength.[46] In pure water, the PSPMA brushes show a fully stretched conformation because of electrostatic repulsion. In KCl electrolyte solution, the polyelectrolyte brushes tend to collapse because of strong electrostatic screening, and part of water was excluded from PSPMA brushes shown in the inset of Figure S2(a) (Supporting Information.[47] Besides, because SPMA was assigned to strong electrolyte, the change of pH has no obvious effect on the PSPMA brushes. This factor has a remarkable effect on the water-absorbing materials for harvesting water. With increasing concentration of KCl solution, more and more Fe_3O_4@SiO_2@PSPMA nanocomposites were needed to harvest a certain amount of KCl solution (50 mg). In contrast, the required amount of nanoparticles had no obvious change as the pH value increased. The effect of ionic strength and pH on the water-absorbing materials had a guiding significance for practical application.

By introduction of charged PSPMA polymer brushes with strong hydration capability, the Fe_3O_4@SiO_2@PSPMA nanocomposites can achieve a good water-absorbing performance like a sponge. Taking advantage of magnetic Fe_3O_4 cores, Fe_3O_4@SiO_2@PSPMA composites with absorbed water can be separated intelligently from the oil/water mixture by an external magnetic field.

4. CONCLUSION

In summary, we developed a novel material, charged polymer brushes-grafted magnetic core–shell–corona composite nanoparticles (Fe_3O_4@SiO_2@PSPMA), to harvest water through the hydration effect and achieve oil–water separation driven by an external magnetic field. The charged polymer brushes, PSPMA

brushes, have both strong hydration capability and good swelling performance, which endow the as-prepared composite nanoparticles with superhydrophilicity and a good water-absorbing performance like a sponge. The SiO_2 shell not only protects Fe_3O_4 cores from damage but also supplies a suitable supporting matrix to immobilize functional groups through numerous surface Si−OH groups. Importantly, the Fe_3O_4@SiO_2@PSPMA nanoparticles with absorbed water can be separated from the oil driven by an external magnetic field. This water-absorbing material uses selective wettability to harvest water and achieve oil−water separation, which is believed to be useful in finding novel approaches for recycling water from sewage and removing water in the petroleum industry.

■ ASSOCIATED CONTENT

Supporting Information

Wettability of the deposited film, water harvesting in dichloromethane, formation of water-holding magnetic beads, water harvesting in hexane, contact angle of an oil droplet on the deposited film in water, cycle test for studying the reusability of the nanocomposites, variation of hydrodynamic diameter, and required amount of nanoparticle as a function of ionic strength or pH, and videos demonstrating the performances of the resultant nanoparticles. This material is available free of charge via the Internet at http://pubs.acs.org.

■ AUTHOR INFORMATION

Corresponding Authors

*E-mail: wangxl@licp.cas.cn.
*E-mail: zhouf@licp.cas.cn.

Notes

The authors declare no competing financial interest.

■ ACKNOWLEDGMENTS

This work was financially supported by the NSFC (21125316, 51305428, 51335010) and Key Research Program of CAS (KJZD-EW-M01).

■ REFERENCES

(1) Sun, T.; Feng, L.; Gao, X.; Jiang, L. Bioinspired Surfaces with Special Wettability. *Acc. Chem. Res.* **2005**, *38*, 644−652.
(2) Lahann, J. Environmental Nanotechnology: Nanomaterials Clean Up. *Nat. Nanotechnol.* **2008**, *3*, 320−321.
(3) Shang, Y.; Si, Y.; Raza, A.; Yang, L.; Mao, X.; Ding, B.; Yu, J. An in Situ Polymerization Approach for the Synthesis of Superhydrophobic and Superoleophilic Nanofibrous Membranes for Oil-Water Separation. *Nanoscale* **2012**, *4*, 7847−7854.
(4) Kota, A. K.; Kwon, G.; Choi, W.; Mabry, J. M.; Tuteja, A. Hygro-Responsive Membranes for Effective Oil-Water Separation. *Nat. Commun.* **2012**, *3*, 1025−1032.
(5) Zhang, L.; Zhang, Z.; Wang, P. Smart Surfaces with Switchable Superoleophilicity and Superoleophobicity in Aqueous Media: Toward Controllable Oil/Water Separation. *NPG Asia Mater.* **2012**, *4*, e8.
(6) Xu, L. P.; Wu, X.; Meng, J.; Peng, J.; Wen, Y.; Zhang, X.; Wang, S. Papilla-Like Magnetic Particles with Hierarchical Structure for Oil Removal from Water. *Chem. Commun.* **2013**, *49*, 8752−8754.
(7) Zhang, F.; Zhang, W. B.; Shi, Z.; Wang, D.; Jin, J.; Jiang, L. Nanowire-Haired Inorganic Membranes with Superhydrophilicity and Underwater Ultralow Adhesive Superoleophobicity for High-Efficiency Oil/Water Separation. *Adv. Mater.* **2013**, *25*, 4192−4198.
(8) Xue, Z.; Wang, S.; Lin, L.; Chen, L.; Liu, M.; Feng, L.; Jiang, L. A Novel Superhydrophilic and Underwater Superoleophobic Hydrogel-Coated Mesh for Oil/Water Separation. *Adv. Mater.* **2011**, *23*, 4270−4273.
(9) Wei, Q. F.; Mather, R. R.; Fotheringham, A. F.; Yang, R. D. Evaluation of Nonwoven Polypropylene Oil Sorbents in Marine Oil-Spill Recovery. *Mar. Pollut. Bull.* **2003**, *46*, 780−783.
(10) Kulawardana, E. U.; Neckers, D. C. Photoresponsive Oil Sorbers. *J. Polym. Sci., Part A: Polym. Chem.* **2010**, *48*, 55−62.
(11) Wang, B.; Guo, Z. pH-Responsive Bidirectional Oil-Water Separation Material. *Chem. Commun.* **2013**, *49*, 9416−9418.
(12) Kwon, G.; Kota, A. K.; Li, Y.; Sohani, A.; Mabry, J. M.; Tuteja, A. On-Demand Separation of Oil-Water Mixtures. *Adv. Mater.* **2012**, *24*, 3666−3671.
(13) Cao, Y.; Zhang, X.; Tao, L.; Li, K.; Xue, Z.; Feng, L.; Wei, Y. Mussel-Inspired Chemistry and Michael Addition Reaction for Efficient Oil/Water Separation. *ACS Appl. Mater. Interfaces* **2013**, *5*, 4438−4442.
(14) Tielrooij, K. J.; Garcia-Araez, N.; Bonn, M.; Bakker, H. J. Cooperativity in Ion Hydration. *Science* **2010**, *328*, 1006−1009.
(15) Panman, M. R.; Bakker, B. H.; Uyl, D. d.; Kay, E. R.; Leigh, D. A.; Buma, W. J.; Brouwer, A. M.; Geenevasen, J. A. J.; Woutersen, S. Water Lubricates Hydrogen-Bonded Molecular Machines. *Nat. Chem.* **2013**, *5*, 929−934.
(16) Klein, J. Hydration Lubrication. *Friction* **2013**, *1*, 1−23.
(17) Gaisinskaya, A.; Ma, L.; Silbert, G.; Sorkin, R.; Tairy, O.; Goldberg, R.; Kampf, N.; Klein, J. Hydration Lubrication: Exploring a New Paradigm. *Faraday Discuss.* **2012**, *156*, 217−233.
(18) Xu, X.; Deng, C.; Gao, M.; Yu, W.; Yang, P.; Zhang, X. Synthesis of Magnetic Microspheres with Immobilized Metal Ions for Enrichment and Direct Determination of Phosphopeptides by Matrix-Assisted Laser Desorption Ionization Mass Spectrometry. *Adv. Mater.* **2006**, *18*, 3289−3293.
(19) Ma, W.; Zhang, Y.; Li, L.; Zhang, Y.; Yu, M.; Guo, J.; Lu, H.; Wang, C. Ti^{4+}-Immobilized Magnetic Composite Microspheres for Highly Selective Enrichment of Phosphopeptides. *Adv. Funct. Mater.* **2013**, *23*, 107−115.
(20) Liu, Z.; Li, M.; Yang, X.; Yin, M.; Ren, J.; Qu, X. The Use of Multifunctional Magnetic Mesoporous Core/Shell Heteronanostructures in a Biomolecule Separation System. *Biomaterials* **2011**, *32*, 4683−4690.
(21) Liu, Z.; Li, M.; Li, Z.; Pu, F.; Ren, J.; Qu, X. Easy Access to Selective Binding and Recyclable Separation of Histidine-Tagged Proteins Using Ni^{2+}-Decorated Superparamagnetic Nanoparticles. *Nano Res.* **2012**, *5*, 450−459.
(22) Luo, B.; Xu, S.; Luo, A.; Wang, W.-R.; Wang, S.-L.; Guo, J.; Lin, Y.; Zhao, D.-Y.; Wang, C.-C. Mesoporous Biocompatible and Acid-Degradable Magnetic Colloidal Nanocrystal Clusters with Sustainable Stability and High Hydrophobic Drug Loading Capacity. *ACS Nano* **2011**, *5*, 1428−1435.
(23) Wang, F.; Pauletti, G. M.; Wang, J.; Zhang, J.; Ewing, R. C.; Wang, Y.; Shi, D. Dual Surface-Functionalized Janus Nanocomposites of Polystyrene/Fe_3O_4@SiO_2 for Simultaneous Tumor Cell Targeting and Stimulus-Induced Drug Release. *Adv. Mater.* **2013**, *25*, 3485−3489.
(24) Li, X.; Li, H.; Liu, G.; Deng, Z.; Wu, S.; Li, P.; Xu, Z.; Xu, H.; Chu, P. K. Magnetite-Loaded Fluorine-Containing Polymeric Micelles for Magnetic Resonance Imaging and Drug Delivery. *Biomaterials* **2012**, *33*, 3013−3024.
(25) Zhu, H.; Shang, Y.; Wang, W.; Zhou, Y.; Li, P.; Yan, K.; Wu, S.; Yeung, K. W.; Xu, Z.; Xu, H.; Chu, P. K. Fluorescent Magnetic Fe_3O_4/Rare Earth Colloidal Nanoparticles for Dual-Modality Imaging. *Small* **2013**, *9*, 2991−3000.
(26) Li, Z.; Dong, K.; Huang, S.; Ju, E.; Liu, Z.; Yin, M.; Ren, J.; Qu, X. A Smart Nanoassembly for Multistage Targeted Drug Delivery and Magnetic Resonance Imaging. *Adv. Funct. Mater.* **2014**, DOI: 10.1002/adfm.201303662.
(27) Zhang, L.; Wu, J.; Wang, Y.; Long, Y.; Zhao, N.; Xu, J. Combination of Bioinspiration: A General Route to Superhydrophobic Particles. *J. Am. Chem. Soc.* **2012**, *134*, 9879−9881.

(28) Tan, K. Y.; Hughes, T. L.; Nagl, M.; Huck, W. T. Nonfouling Capture-Release Substrates Based on Polymer Brushes for Separation of Water-Dispersed Oil Droplets. *ACS Appl. Mater. Interfaces* **2012**, *4*, 6403−6409.
(29) Kobayashi, M.; Terayama, Y.; Yamaguchi, H.; Terada, M.; Murakami, D.; Ishihara, K.; Takahara, A. Wettability and Antifouling Behavior on the Surfaces of Superhydrophilic Polymer Brushes. *Langmuir* **2012**, *28*, 7212−7222.
(30) Farrukh, A.; Akram, A.; Ghaffar, A.; Hanif, S.; Hamid, A.; Duran, H.; Yameen, B. Design of Polymer-Brush-Grafted Magnetic Nanoparticles for Highly Efficient Water Remediation. *ACS Appl. Mater. Interfaces* **2013**, *5*, 3784−3793.
(31) Yan, J.; Li, B.; Yu, B.; Huck, W. T.; Liu, W.; Zhou, F. Controlled Polymer-Brush Growth from Microliter Volumes Using Sacrificial-Anode Atom-Transfer Radical Polymerization. *Angew. Chem., Int. Ed.* **2013**, *52*, 9125−9129.
(32) Li, B.; Yu, B.; Huck, W. T.; Zhou, F.; Liu, W. Electrochemically Induced Surface-Initiated Atom-Transfer Radical Polymerization. *Angew. Chem., Int. Ed.* **2012**, *51*, 5092−5095.
(33) Zheng, J.; Dong, Y.; Wang, W.; Ma, Y.; Hu, J.; Chen, X.; Chen, X. In Situ Loading of Gold Nanoparticles on Fe_3O_4@SiO_2 Magnetic Nanocomposites and Their High Catalytic Activity. *Nanoscale* **2013**, *5*, 4894−4901.
(34) Jeong, U.; Teng, X.; Wang, Y.; Yang, H.; Xia, Y. Superparamagnetic Colloids: Controlled Synthesis and Niche Applications. *Adv. Mater.* **2007**, *19*, 33−60.
(35) Tan, H.; Xue, J. M.; Shuter, B.; Li, X.; Wang, J. Synthesis of Peolated Fe_3O_4@SiO_2 nanoparticles Via Bioinspired Silification for Magnetic Resonance Imaging. *Adv. Funct. Mater.* **2010**, *20*, 722−731.
(36) Lu, A. H.; Salabas, E. L.; Schuth, F. Magnetic Nanoparticles: Synthesis, Protection, Functionalization, and Application. *Angew. Chem., Int. Ed.* **2007**, *46*, 1222−1244.
(37) Li, B.; Yu, B.; Huck, W. T.; Liu, W.; Zhou, F. Electrochemically Mediated Atom Transfer Radical Polymerization on Nonconducting Substrates: Controlled Brush Growth through Catalyst Diffusion. *J. Am. Chem. Soc.* **2013**, *135*, 1708−1710.
(38) Liu, X.; Ye, Q.; Song, X.; Zhu, Y.; Cao, X.; Liang, Y.; Zhou, F. Responsive Wetting Transition on Superhydrophobic Surfaces with Sparsely Grafted Polymer Brushes. *Soft Matter* **2011**, *7*, 515−523.
(39) Husseman, M.; Malmström, E. E.; McNamara, M.; Mate, M.; Mecerreyes, D.; Benoit, D. G.; Hedrick, J. L.; Mansky, P.; Huang, E.; Russell, T. P.; Hawker, C. J. Controlled Synthesis of Polymer Brushes by "Living" Free Radical Polymerization Techniques. *Macromolecules* **1999**, *32*, 1424−1431.
(40) Chen, H.; Deng, C.; Zhang, X. Synthesis of Fe_3O_4@SiO_2@PMMA Core-Shell-Shell Magnetic Microspheres for Highly Efficient Enrichment of Peptides and Proteins for MALDI-ToF MS Analysis. *Angew. Chem., Int. Ed.* **2010**, *49*, 607−611.
(41) Liu, J.; Xu, J.; Che, R.; Chen, H.; Liu, M.; Liu, Z. Hierarchical Fe_3O_4@TiO_2 Yolk-Shell Microspheres with Enhanced Microwave-Absorption Properties. *Chem.—Eur. J.* **2013**, *19*, 6746−6752.
(42) Zhang, Y.; Yang, Y.; Ma, W.; Guo, J.; Lin, Y.; Wang, C. Uniform Magnetic Core/Shell Microspheres Functionalized with Ni^{2+}-Iminodiacetic Acid for One Step Purification and Immobilization of His-Tagged Enzymes. *ACS Appl. Mater. Interfaces* **2013**, *5*, 2626−2633.
(43) Ma, W.; Xu, S.; Li, J.; Guo, J.; Lin, Y.; Wang, C. Hydrophilic Dual-Responsive Magnetite/PMMA Core/Shell Microspheres with High Magnetic Susceptibility and pH Sensitivity Via Distillation-Precipitation Polymerization. *J. Polym. Sci., Part A: Polym. Chem.* **2011**, *49*, 2725−2733.
(44) Shao, M.; Ning, F.; Zhao, J.; Wei, M.; Evans, D. G.; Duan, X. Preparation of Fe_3O_4@SiO_2@Layered Double Hydroxide Core-Shell Microspheres for Magnetic Separation of Proteins. *J. Am. Chem. Soc.* **2012**, *134*, 1071−1077.
(45) Kim, J.; Kim, H. S.; Lee, N.; Kim, T.; Kim, H.; Yu, T.; Song, I. C.; Moon, W. K.; Hyeon, T. Multifunctional Uniform Nanoparticles Composed of a Magnetite Nanocrystal Core and a Mesoporous Silica Shell for Magnetic Resonance and Fluorescence Imaging and for Drug Delivery. *Angew. Chem., Int. Ed.* **2008**, *47*, 8438−8441.
(46) Wei, Q.; Cai, M.; Zhou, F.; Liu, W. Dramatically Tuning Friction Using Responsive Polyelectrolyte Brushes. *Macromolecules* **2013**, *46*, 9368−9379.
(47) Zhou, F.; Shu, W.; Welland, M. E.; Huck, W. T. S. Highly Reversible and Multi-Stage Cantilever Actuation Driven by Polyelectrolyte Brushes. *J. Am. Chem. Soc.* **2006**, *128*, 5326−5327.